Supplementary Information for

Dual-Target, High-Capacity Removal of Microplastics and Dyes from Water by a Recyclable Sponge Monolith

*Ting Huang[1, #], Fangtian Liu[1, #], Yifei Liu[1], Bingchen Wu[1], Xiaowen Shi[1], Yang Wu[1, *], Hongbing Deng[1, *], Xue Zhou[2, *]*

[1]Hubei Key Laboratory of Biomass Resource Chemistry and Environmental Biotechnology, Hubei International Scientific and Technological Cooperation Base of Sustainable Resource and Energy, Hubei Engineering Center of Natural Polymers-based Medical Materials, School of Resource and Environmental Science, Wuhan University, Wuhan 430079, China.

[2]Key Laboratory of Environment and Health, Ministry of Education, Department of Occupational and Environmental Health, School of Public Health, Tongji Medical College, Huazhong University of Science and Technology, Wuhan, 430030, China

[#] These authors contributed equally to this work.

* Corresponding authors.

Email: youngwuu@whu.edu.cn (Y. Wu); hbdeng@whu.edu.cn (H. Deng); xue.zhou@hust.edu.cn (X. Zhou).

Keywords: chitin; microplastic; dye; co-removal; wastewater treatment

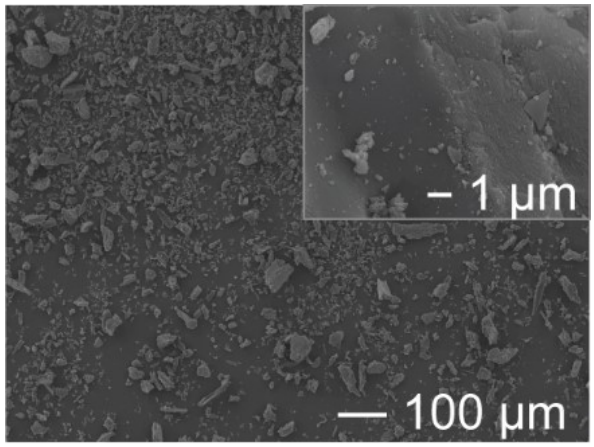

Fig. S1. SEM of AC (400 mesh).

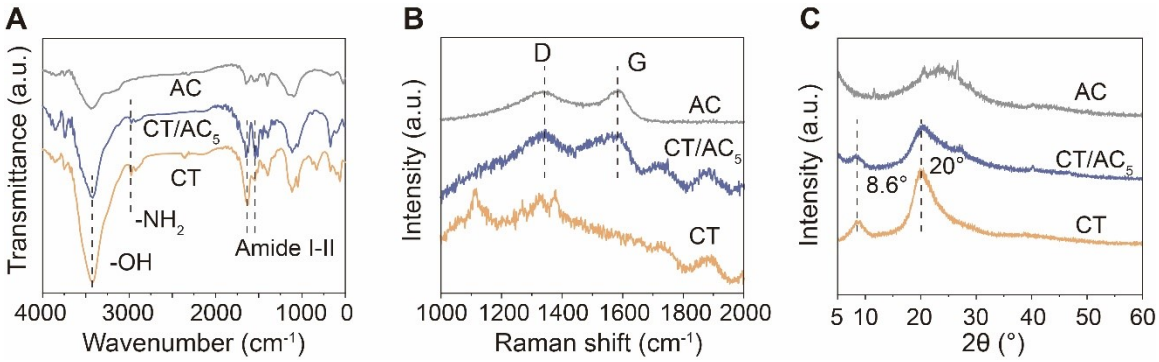

Figure S2. (A) FTIR, (B) Raman and (C) XRD spectra of CT/AC$_5$ sponge, CT sponge and AC.

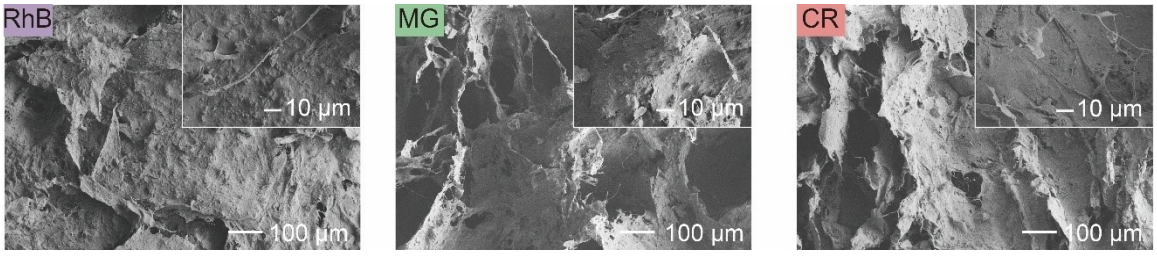

Figure S3. SEM of CT/AC_5 adsorbing (a) RhB, (b) MG, and (c) CR.

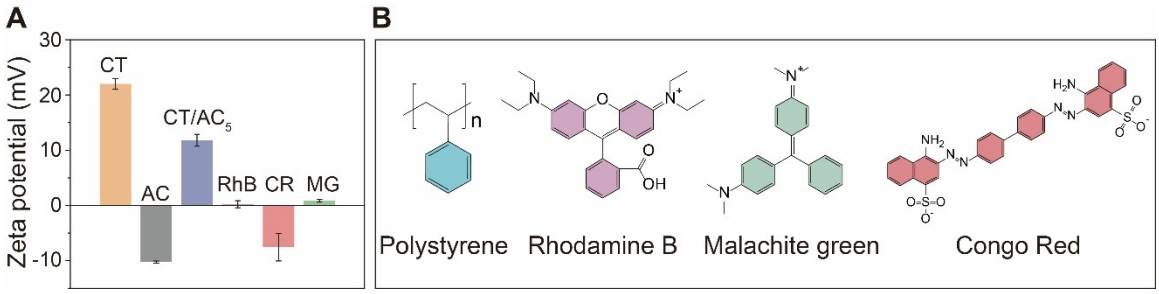

Figure S4. (a) Zeta potentials of CT, AC, CT/AC_5 and pollutants. (b) Structural formulas of PS, RhB, MG, and CR.

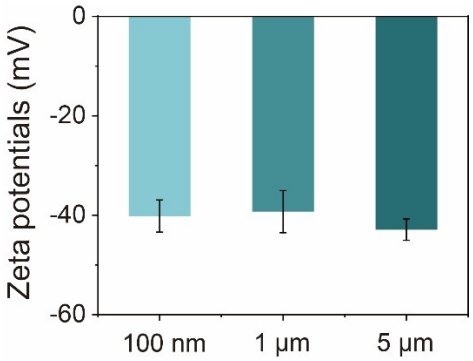

Figure S5. Zeta potentials of PS with different size.

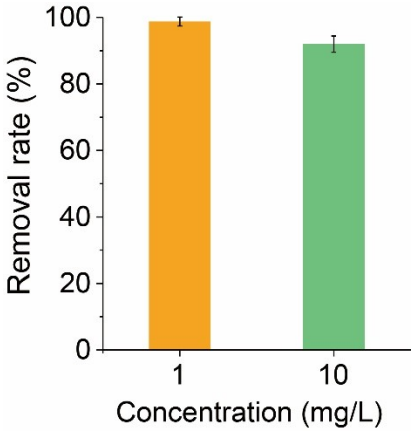

Figure S6. The 5 μm PS removal rate of CT/AC_5 at the concentration of environment levels (1 and 10 mg/L).

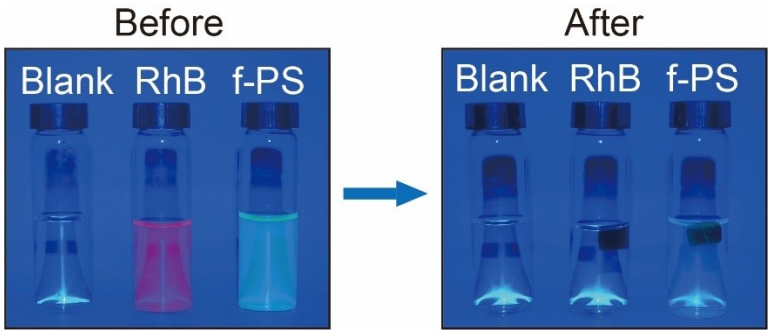

Figure S7. Photos of RhB and fluorescent-PS (f-PS) before and after CT/AC_5 treatment under UV light.

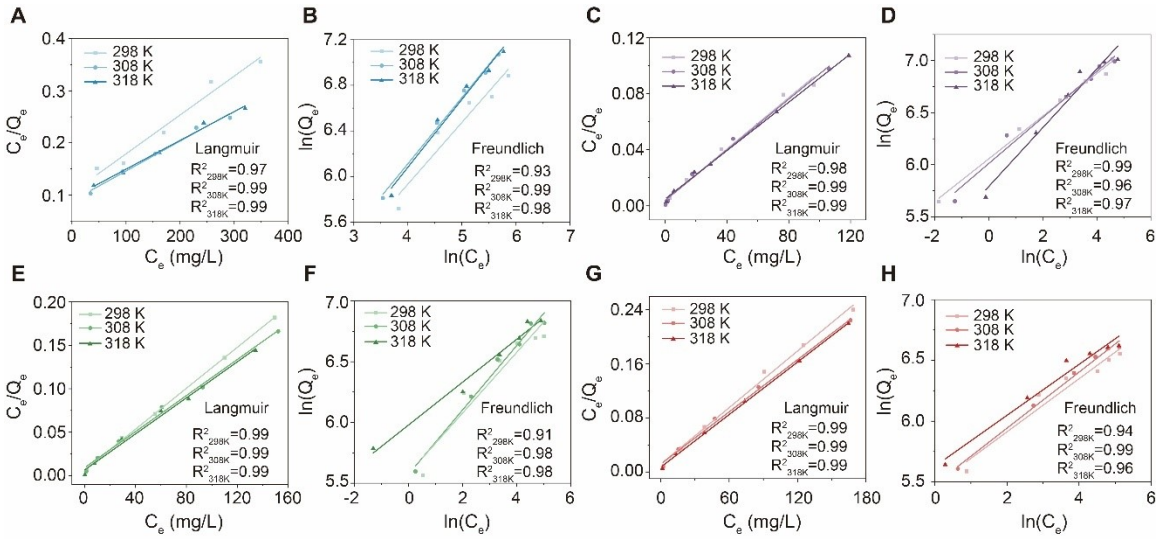

Figure S8. Adsorption isotherms fitted by Langmuir and Freundlich models for adsorption of (A, B) PS microsphere, (C, D) RhB, (E, F) MG, and (G, H) CR on CT/AC$_5$.

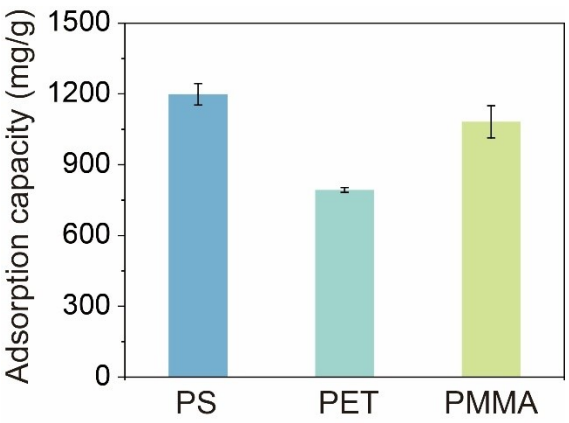

Figure S9. Adsorption capacity of PET and PMMA of CT/AC$_5$.

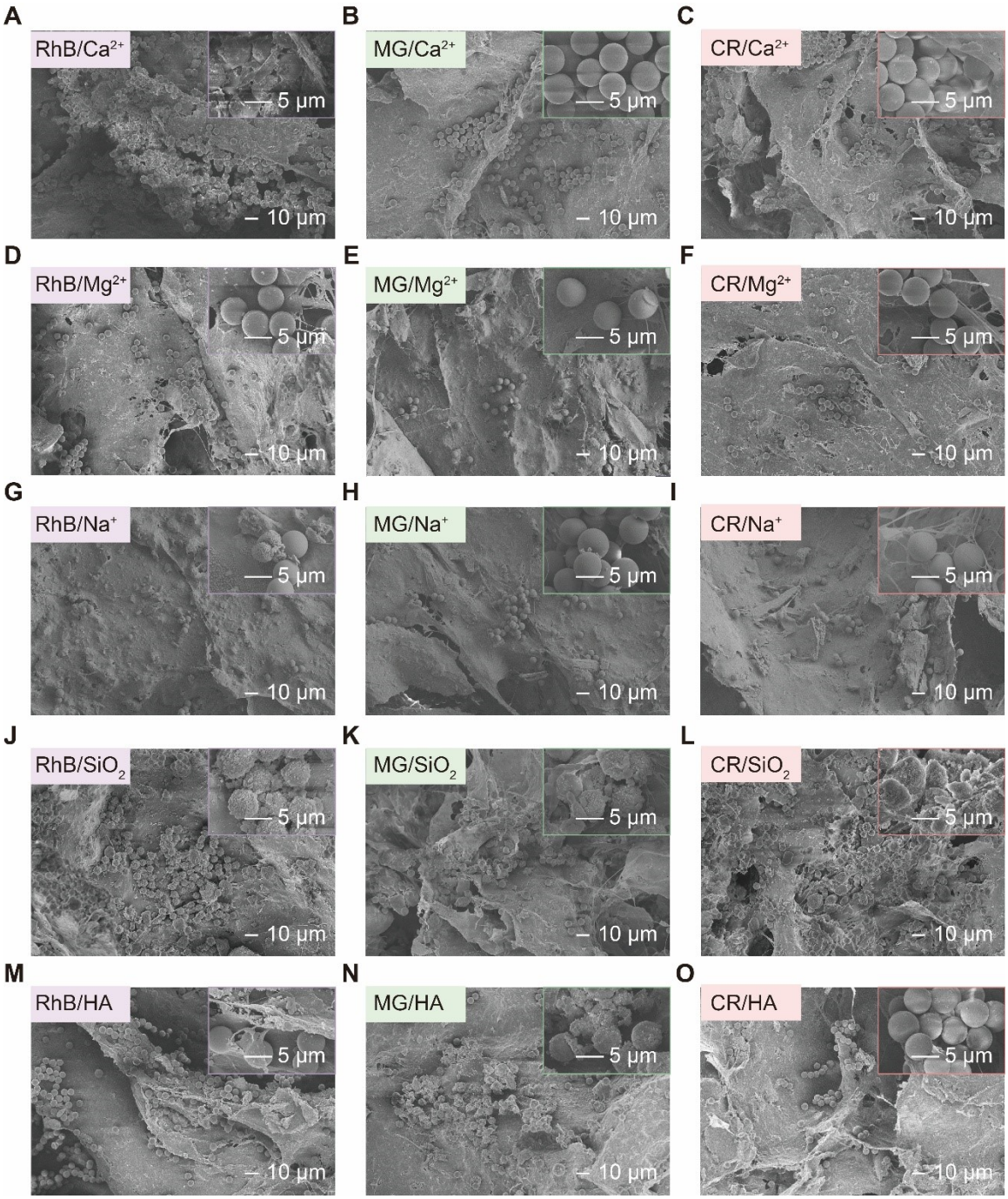

Figure S10. SEM of CT/AC_5 for binary pollutants under the influence of different factors. (A-C) Ca^{2+}, (D-F) Mg^{2+}, (G-I) Na^{+}, (J-L) SiO_2, (M-O) HA. The concentration of metal ions and humic acid was 30 ppm, and the concentration of SiO_2 was 250 ppm.

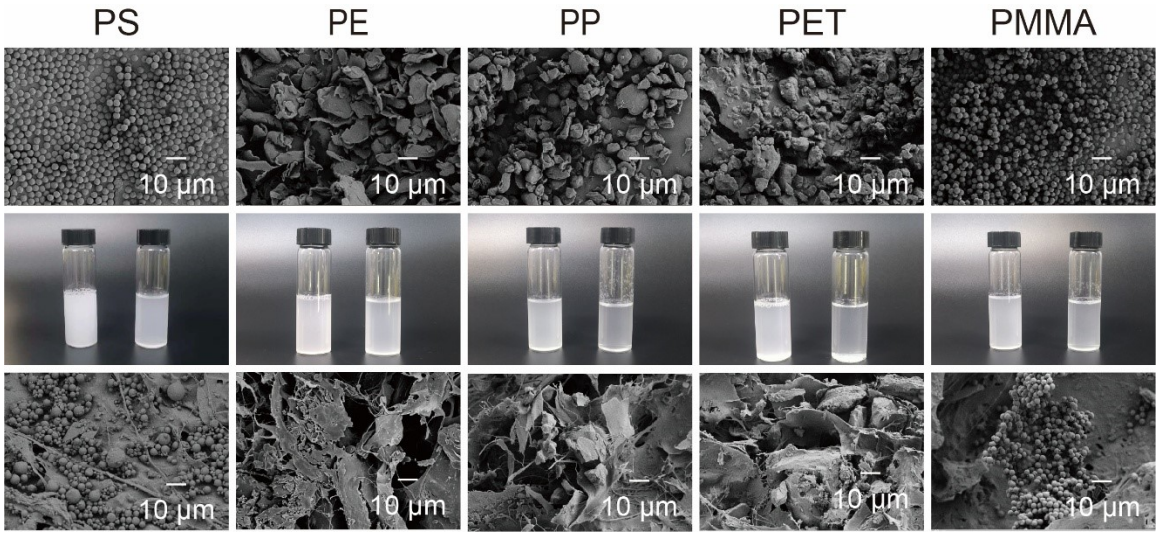

Figure S11. SEM images of different MPs (PS, PE, PP, PET, and PMMA), the solvent before and after CT/AC_5 treatment, and the morphology of CT/AC_5 after adsorption.

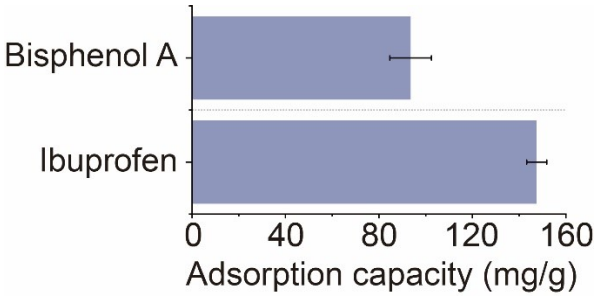

Figure S12. Adsorption capacity of CT/AC_5 for bisphenol A and Ibuprofen.

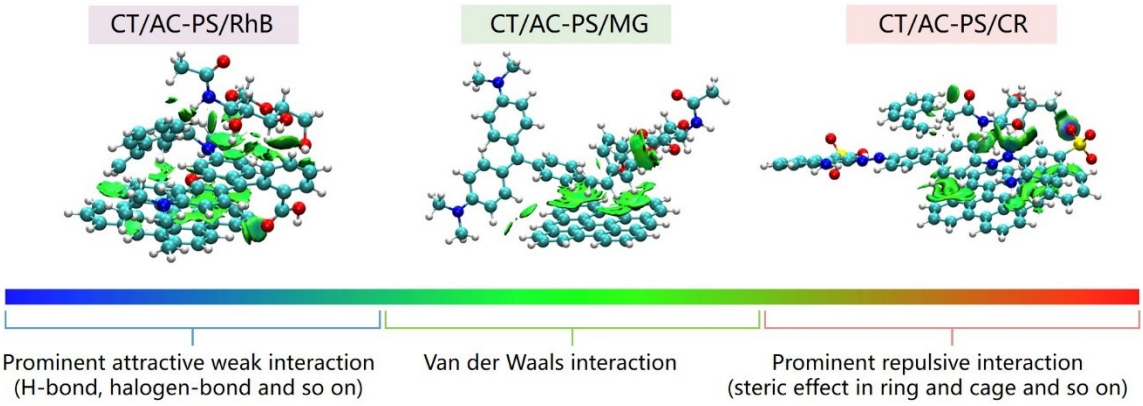

Figure S13. IGMH-based non-covalent interaction analysis between CT/AC and PS and dyes (PS/RhB, PS/MG, and PS/CR).

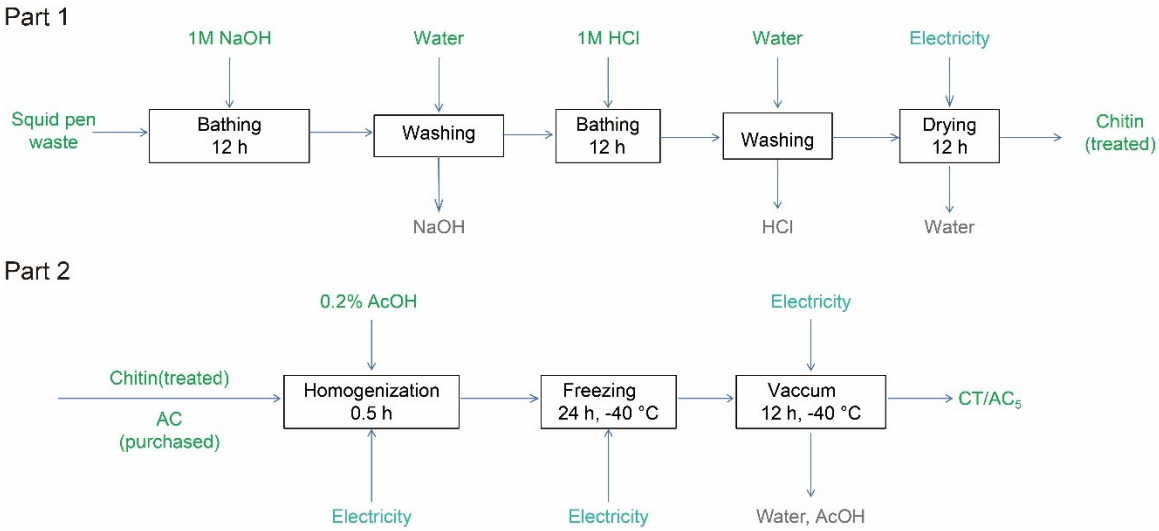

Figure S14. Unit processes for chitin extraction and CT/AC_5 sponge preparation.

Table S1. The scoring criteria of CT/AC, CT, granular AC, and AC in terms of adsorption capacity, economy, sustainability, environmental tolerance, and recyclability.

Sample	Adsorption capacity	Economy	Sustainability	Environmental tolerance	Recyclability
CT	5	8	6	5	7
CT/AC	9	9	9	9	9
GAC	2	7	4	8	7
AC	6	9	4	8	5

We compared the CT/AC with CT, GAC, and AC in terms of adsorption capacity, economy, sustainability, environmental tolerance, and recyclability. The evaluation and scoring of CT, CT/AC, GAC, and AC were conducted based on the experimental results obtained.

In terms of adsorption capacity, CT showed exceptional uptake for PS microplastics (800.23 mg/g) and CR (635.75 mg/g), along with moderate adsorption for RhB (40.10 mg/g) and MG (154.35 mg/g). The CT/AC exhibited significantly enhanced performance, achieving 1177.17 mg/g for PS, 1038.86 mg/g for RhB, 911.23 mg/g for MG, and 734.47 mg/g for CR. In contrast, GAC displayed very low adsorption across all tested pollutants, with values of only 2.43 mg/g for PS and 4.10-14.86 mg/g for the dyes. AC showed moderate adsorption for PS (102.43 mg/g) but relatively high capacities for RhB (735.65 mg/g), MG (615.26 mg/g), and CR (544.74 mg/g). In conclusion, CT exhibited superior adsorption for PS and CR, whereas AC was more effective for general dye removal. The CT/AC composite successfully integrated the benefits of both components, while GAC displayed limited adsorption capacity, likely due to its poor dispersion.

CT was derived from waste squid pen biomass and required a simple fabrication process. Both GAC and AC were low-cost materials, but their preparation involved energy-intensive steps such as high-temperature treatment and steam activation. CT/AC was

composed of AC and waste-derived CT, offering economic advantages due to the low cost of raw materials and the simplicity of its fabrication.

CT exhibited good sustainability in post-treatment processes, such as cyclic adsorption and integrated hot-pressing. In contrast, the fabrication of AC and GAC was energy-intensive. CT/AC was composed of waste-derived biopolymer (CT) and AC, demonstrating strong sustainability through its reusability, potential for hot-pressing regeneration, and high-value conversion. LCA results further indicated that CT/AC had a lower carbon footprint compared to the other materials.

In terms of environmental tolerance, AC and GAC possessed granular hardness, which maintained stable adsorption capacity in polluted water. CT provided a soft and flexible framework but lacked mechanical strength. In comparison, CT/AC exhibited robust mechanical performance in harsh environment.

Recyclability: GAC and CT showed good recoverability due to their hard granular or bulk form, whereas AC showed limited recovery ability because of its powdery form. CT/AC overcame the limitation of powder and offered a unique and efficient regeneration pathway.

Table S2. The specific surface area, pore volume, average pore diameter and micropore volume of CT/AC_5 sponge, CT sponge and AC.

Parameter	Unit	CT sponge	CT/AC_5	AC
BET specific surface area	m^2/g	36.60	552.80	1234.20
Total pore volume	cm^3/g	0.05	0.58	1.21
Average pore diameter	nm	5.42	4.20	3.94
Micropore volume (MP-plot)	cm^3/g	0.01	0.14	0.33

Table S3. Overview of main adsorption experiments conducted in this study.

Experiment type	Pollutants	C (ppm)	Dosage (mg)/ Volume (ml)	*T* (K)/ Equilibrium time(h)
Dyes removal	RhB, MG, CR, MB, MO, CV	200	3.5/20	298/24
PS removal	PS (100, 500, 1000, 3000, 5000 nm)	500	3.5/20	298/24
Batch under different initial concentration	PS, Dyes (RhB, MG, CR)	PS: 100, 200, 300, 400, 500 Dyes: 50, 100, 150, 200, 250, 300	3.5/20	298/24
Adsorption kinetics	PS, Dyes (RhB, MG, CR)	PS: 500 Dyes: 250	3.5/20	298/48
Adsorption isotherm	PS, Dyes (RhB, MG, CR)	PS: 100, 200, 300, 400, 500 Dyes: 50, 100, 150, 200, 250, 300	3.5/20	298/24, 308/24, 318/24
Batch removal under different pH	PS, Dyes (RhB, MG, CR)	PS: 500 Dyes: 250	3.5/20	298/24
Batch removal under different salt concentration	PS, Dyes (RhB, MG, CR)	PS: 500 Dyes: 250	3.5/20	298/24
MPs removal	PS, PE, PP, PET, PMMA	500	3.5/20	298/24
Antibiotic removal	Ibuprofen, Bisphenol A	100	3.5/20	298/24
Batch removal of binary pollutants at different condition	PS/RhB, PS/MG, PS/CR	PS:500 Dyes:250	3.5/20	298/24
Dynamic adsorption removal of binary pollutants	PS/RhB, PS/MG, PS/CR	PS:20 Dyes:20	1000/500	298/24

Where *T* (K) is the absolute temperature.

Table S4. Relevant kinetic parameters fitted by the pseudo-first-order and pseudo-second-order adsorption kinetic models.

Pseudo-first-order model				Pseudo-second-order model		
Pollutants	q_e (mg/g)	k_1 (g/mg min)	R^2	q_e (mg/g)	k_2 (g/mg min)	R^2
PS	1036.70	1.30×10^{-3}	0.98	1250.00	2.86×10^{-3}	0.94
RhB	633.08	1.60×10^{-3}	0.97	1111.11	1.04×10^{-2}	0.99
MG	499.85	1.70×10^{-3}	0.94	909.09	5.50×10^{-3}	0.98
CR	648.39	1.30×10^{-3}	0.93	769.23	1.04×10^{-2}	0.99

The data obtained from the analysis of pseudo-first-order kinetic model (S1) and pseudo-second-order kinetic model (S2) were calculated according to the following equations:

$$\ln(q_e - q_t) = \ln(q_e) - k_1 t \quad \text{(S1)}$$

$$\frac{t}{q_t} = \frac{1}{k_2 q_e^2} + \frac{t}{q_e} \quad \text{(S2)}$$

where k_1 (g/mg min) and k_2 (g/mg min) are the rate constants of pseudo-first-order and pseudo-second-order model, respectively; q_e and q_t (mg/g) are the pollutant uptake at equilibrium and at time t min, respectively.

Table S5. Intraparticle diffusion model parameters.

Pollutants	k_{i1}	k_{i2}	k_{i3}	C_{i1}	C_{i2}	C_{i3}	R_1^2	R_2^2	R_3^2
PS	32.33	14.65	214.83	96.11	249.36	18.95	0.95	0.92	0.89
RhB	61.12	24.17	5.25	67.06	352.98	820.63	0.92	0.99	0.99
MG	59.91	21.74	5.82	129.55	176.84	569.90	0.99	0.98	0.88
CR	28.04	15.93	5.86	99.93	181.15	467.11	0.87	0.99	0.72

The data obtained from the analysis of the intra-particle diffusion model(S3) were calculated according to the following equation:

$$q_t = k_{id} t^{0.5} + C \quad \text{(S3)}$$

where k_{id} (mg/g $min^{1/2}$) is the rate constant of intra-particle diffusion model; q_t(mg/g) is the uptake at time t; C (mg/g) is intercept which can reflect the boundary layer thickness.

Table S6. The relevant parameters were determined according to Langmuir and Freundlich models.

	Langmuir model				Freundlich model		
Pollutants	T (K)	q_m (mg/g)	k_L (L/g)	R^2	k_f (mg/g)	n (g/L)	R^2
PS	298	1340.30	7.20×10^{-3}	0.99	42.96	1.84	0.93
	308	1519.76	7.20×10^{-3}	0.99	44.03	1.72	0.99
	318	1666.67	6.70×10^{-3}	0.99	40.28	1.68	0.98
RhB	298	1092.93	0.23	0.98	426.44	4.88	0.98
	308	1106.92	0.24	0.99	326.69	3.54	0.96
	318	1159.31	0.18	0.99	407.65	4.52	0.97
MG	298	847.46	0.19	0.99	264.56	4.01	0.91
	308	961.54	0.11	0.99	263.10	3.78	0.98
	318	961.54	0.16	0.99	394.79	5.67	0.98
CR	298	714.29	0.12	0.99	238.82	4.58	0.94
	308	775.19	0.11	0.99	240.06	4.33	0.99
	318	769.23	0.18	0.99	278.29	4.77	0.96

The data obtained by using Langmuir (S4) and Freundlich (S5) models to explain the adsorption isotherm was shown in Table S5.

$$\frac{\gamma_e}{q_e} = \frac{1}{K_L q_m} + \frac{\gamma_e}{q_m} \quad \text{(S4)}$$

$$lnq_e = lnk_F + \frac{1}{n} lnC_e \quad \text{(S5)}$$

where T (K) is the absolute temperature, q_e (mg/g) is the equilibrium uptake, q_m (mg/g) is the maximum uptake capacity, γ_e (mg/L) is the concentration of pollutants at adsorption equilibrium.

Table S7. Thermodynamic parameters of pollutants adsorption to CT/AC$_5$.

Pollutants	Temperature (K)	ΔG (KJ/mol)	ΔS (J/mol)	ΔH (KJ/mol)
PS	298	-2.56	65.34	16.80
	308	-3.57		
	318	-4.47		
RhB	298	-5.90	8.41	8.57
	308	-5.96		
	318	-6.07		
MG	298	-4.22	44.85	9.17
	308	-4.60		
	318	-5.12		
CR	298	-3.53	23.91	3.58
	308	-3.82		
	318	-4.00		

In order to further study the thermodynamic mechanism of adsorption, the standard Gibbs free energy change (ΔH) and standard entropy change (ΔS) were calculated using the following formulas (S6), (S7), (S8).

$$k_d = \frac{q_e}{\gamma_e} \quad \text{(S6)}$$

$$\Delta G = -RT ln k_d \quad \text{(S7)}$$

$$ln k_d = \frac{\Delta S}{R} - \frac{\Delta H}{RT} \quad \text{(S8)}$$

where R (8.314 J/mol K) is the universal gas constant, k_d (mL/g) is the distribution coefficient, γ_e (mg/L) is the concentration of pollutants at adsorption equilibrium, and q_e (mg/g) is the pollutants adsorption capacity at equilibrium.

Table S8. Cost calculation for adsorbent.

Materials	Reagent	Main processes	Cost ($)/g
ChGO	Chitin, NaOH, Urea, Epichlorohydrin (ECH), Ethanol, Graphene oxide	Ultrasound 20 min Freezing 16 h Lyophilization 48 h 4℃ gelation 24 h	454.54-710.28
ChCB	Chitin, Carbon black, NaOH, Urea, Epichlorohydrin, Ethanol	Freezing-thawing cycle Lyophilization 48 h	0.07-0.11
GO/CS/GP	Chitosan, Graphene oxide, Genipin, Acetic acid, NaOH, Ethanol	Ultrasound 20 min Freezing 24 h Lyophilization 72 h	68.29-123.00
PDA-MCS	Chitosan, Dopamine hydrochloride, Magnetic Fe_3O_4 nanoparticles, ethanol	String 2 h Freezing 24 h Lyophilization 48 h	4.29-8.71
PDMS@ZIF-67/CS	2-Methylimidazole, Co $(NO_3)_2 \cdot 6H_2O$, Chitosan, Polydimethylsiloxane, NaOH, Acetic acid	Carbonization 11 h Freezing 12 h Lyophilization 24 h	0.50-0.64
CT/AC_5	Chitin, AC, Acetic acid	String 2 h Freezing 12 h Lyophilization 24 h	0.02-0.06

Table S9. Comparison of parameters with other adsorbents.

Materials	MPs	Dosage	C (ppm)	Q (mg/g)	Cost ($)/g	Ref
ChGO	PS PS-COOH PS-NH_2 PS (1 μm)	1 cm^3	20	8.51 ± 0.60	454.54-710.28	1
ChCB	PS (1 μm)	20 mg	20	99.74 ± 2.0	0.07-0.11	2
GO/CS/GP	PS (1 μm)	0.01 g/20 ml	10	7.42 ± 0.7	68.29-123.00	3
PDA-MCS	PET PE PS (10-200 nm)	-	300	125 ± 17	4.29-8.71	4
PDMS@ZIF-67/CS	PS (488 nm)	1 cm^3/10 ml	600	34.5	0.50-0.64	5
CT/AC_5	PS (100, 500, 1000, 3000, 5000 nm), PE, PP, PET, and PMMA	3.5 mg/20 ml	500	1249.41 ± 53.83	0.02-0.06	This work

Table S10. The key operational parameters of fixed-bed adsorption apparatus.

Parameters	
Fixed-bed height	20 cm
Influent flow rate	50 rpm
Contact time	4 h

Table S11. Life cycle assessment checklist

Comment	Component	Amount	Unit	Source/Provider
-	Squid pen waste	1.61	kg	Waste input
1 M,15.28 L	NaOH	1.29	kg	Sodium hydroxide, without water, in 50% solution state | market for | APOS, S
1 M,14.42 L	HCl	1.96	kg	Hydrochloric acid, without water, in 30% solution state | market for | APOS, U
-	AC	0.50	kg	Activated carbon, granular | activated carbon production, granular from hard coal | APOS, S
-	AcOH	0.20	kg	Acetic acid, without water, in 98% solution state | acetaldehyde oxidation | APOS, S
-	Water for dilution	30	L	Tap water | tap water production, ultrafiltration treatment | APOS, S
-	Water for sponge production	99.80	L	
1.02 kW, 24 h	Electricity for stirring	24.48	kWh	Electricity, low voltage {CN}| market group for | APOS, S
0.5 kW, 12 h	Electricity for drying	6	kWh	
4.0 kW, 0.5 h	Electricity for homogenization	2	kWh	
0.09 kW, 24 h	Electricity for freezing	2.16	kWh	
37 kW, 12 h	Electricity for vacuum drying	444	kWh	
185 km	transport, freight, lorry	-	kg km	Transport, freight, lorry, unspecified | transport, freight, lorry, all sizes, EURO6 to generic market for | APOS, S
-	biowaste	1.11	kg	Biowaste | treatment of biowaste, industrial composting | APOS, S
-	wastewater	30	L	Wastewater, unpolluted | treatment of, capacity 5E9l/year | APOS, S
-	wastewater	99.80	L	
-	CT/AC_5	1	kg	Output materials

Supplementary References

(1) C. Sun, Z. Wang, L. Chen, F. Li, *Chem. Eng. J.* 2020, **393**, 124796.

(2) Z. Zhu, X. Wu, C. Wang, Z. Meng, C. Sun, Z. Wang, *Sep. Purif. Technol.* 2023, **322**, 124321.

(3) M. Ko, T. Jang, S. Yoon, J. Lee, J. H. Choi, J. W. Choi, J. A. Park, *Chemosphere* 2024, **356**, 141956.

(4) B. Zheng, B. Li, H. Wan, X. Lin, Y. Cai, *J. Hazard. Mater.* 2022, **431**, 128611.

(5) F. Liang, Y. Xu, S. Chen, Y. Zhu, Y. Huang, B. Fei, W. Guo, *ACS Appl. Mater. Interfaces* 2022, **14**, 56027-56045.